Journal of Archaeological Science: Reports 20 (2018) 307–323

Contents lists available at ScienceDirect

Journal of Archaeological Science: Reports

journal homepage: www.elsevier.com/locate/jasrep

A novel interdisciplinary approach for building archaeology: The integration of mortar "single grain" luminescence dating into archaeological research, the example of Saint Seurin Basilica, Bordeaux

P. Urbanová[a,*], A. Michel[b], N. Cantin[a], P. Guibert[a], P. Lanos[c], P. Dufresne[c], L. Garnier[c]

[a] IRAMAT-CRP2A, "Institut de Recherche sur les ArchéoMATériaux - Centre de Recherche en Physique Appliquée à l'Archéologie", UMR5060 CNRS-Université de Bordeaux-Montaigne, Maison de l'Archéologie, Esplanade des Antilles, 33607 Pessac Cedex, France
[b] Ausonius, "Institut de Recherche - Antiquité et Moyen Age ", UMR 5607 CNRS-Université de Bordeaux-Montaigne, Maison de l'Archéologie, Esplanade des Antilles, 33607 Pessac Cedex, France
[c] IRAMAT-CRP2A, "Institut de Recherche sur les ArchéoMATériaux - Centre de Recherche en Physique Appliquée à l'Archéologie", Géosciences-Rennes, UMR 6118 Université Rennes 1, Campus de Beaulieu, Bât. 15, CS 74205 - 35042 Rennes Cedex, France

ARTICLE INFO

Keywords:
Single grain OSL dating
Lime mortar
Brick
Charcoal
Construction
Early medieval
Building archaeology

ABSTRACT

This paper deals with new strategies for dating the construction of ancient monuments, one of the most topical issues in archaeology. Our approach is demonstrated by the study of an emblematic early medieval Basilica *Saint Seurin* in Bordeaux whose oldest building phases have never been well-understood and dated before due to the lack of written sources and archaeological findings. We mainly focus on the analyses of mortar as an omnipresent and non-recyclable material whose making is undoubtedly contemporary to the building process. For the first time, we integrated a novel, recently validated protocol for dating historical mortar through optically stimulated luminescence using the « single grain technique » (SG-OSL) into archaeological research.

The present work arises from close and continuous collaboration between archaeologists and archaeometers both in situ and during post-excavation analyses. SG-OSL dating of mortar, as the most innovative aspect of the study, was combined with mortar characterization, radiocarbon dating of charcoals and partly also with archaeomagnetic and thermoluminescence dating of bricks for a cross-check of chronological data.

We identified and dated several independent building phases in the crypt of the present church where mortar was the only building material preserved. By combining physical dating methods with stratigraphic constraints based on archaeological interpretations, all the findings were used to construct a chronological model that proves continuity in occupation of the site between the 5th and the 12th centuries, reflecting its high cultural and symbolic value.

By the inter-connection of mortar dating by SG-OSL with archaeology and other fields of archaeometry, we set up a renewed interdisciplinary working model for building archaeology that opens interesting perspectives for the future of this research field.

1. Introduction

Accurate dating of historical buildings still poses a challenge in the field of building archaeology. In particular, and often for early medieval constructions, no literary sources exist and no archaeological finds (coins, ceramic fragments) or organic remains allowing typo-chronological or radiocarbon dating respectively, are available. In better cases, they exist but give only an indirect or an uncertain chronological clue in relation to the building process. Such circumstances make it difficult to interpret many ancient buildings in a wider historical context.

The Saint Seurin Basilica in Bordeaux which we present in our research approach is a typical demonstration of the difficulties archaeologists often deal with when studying early medieval architecture:

- Very few historical sources
- Use of *spolia* and repeated reconstructions of the primitive building
- Archaeological reports from the 19th and 20th century insufficiently detailed to understand previous excavations and their effect on the integrity of the archaeological remains

The challenge of the present paper is to demonstrate how to get

* Corresponding author.
E-mail address: urbanpetra@seznam.cz (P. Urbanová).

https://doi.org/10.1016/j.jasrep.2018.04.009
Received 23 October 2017; Received in revised form 9 April 2018; Accepted 10 April 2018
Available online 21 May 2018
2352-409X/ © 2018 The Authors. Published by Elsevier Ltd. This is an open access article under the CC BY-NC-ND license (http://creativecommons.org/licenses/BY-NC-ND/4.0/).

further in understanding construction history of the site despite such a lack of chronological information. Its principal contribution consists in a novel approach for mortar dating through optically stimulated luminescence using the “single grain technique”.

Mortar is the most suitable element for dating a construction since its making is contemporary to the building process. Archaeologists recognized the importance of mortar analyses many years ago (Frizot, 1975; Furlan & Bissenger, 1975; Sapin, 1991) and characterization studies of mortars that may help in some cases to distinguish different construction phases have become widespread (e.g. (Büttner, 2014; Carò et al., 2008; Chiarelli et al., 2015; De Luca et al., 2013; Miriello et al., 2010; Sanjurjo-Sánchez et al., 2010; Vendrell-Saz et al., 1996)). Until recently, the question of mortar dating has been especially linked to radiocarbon analyses of carbonation that has been under research since the 60s' (Labeyrie & Delibrias, 1964). Despite many different solutions tested in recent years (Hajdas et al., 2017; Hayen et al., 2017; Heinemeier et al., 1997; Heinemeier et al., 2010; Lindroos et al., 2007; Marzaioli et al., 2013; Nawrocka et al., 2005; Ortega et al., 2012; Pesce & Ball, 2000; Ringbom et al., 2011), ^{14}C dating of the carbonation process in mortar remains complicated. None of the current experimental procedures can be used universally for the dating of mortars originating from buildings of unknown age, without having an independent age control.

An alternative approach for mortar dating consists in the use of optically stimulated luminescence (OSL) which is applied on the quartz sand extracted from the mortar and not on the binder. OSL allows the dating of the last exposure of the mortar aggregate to light and this corresponds to the moment of mortar making. This application was first tested in 2000 (Bøtter-Jensen et al., 2000) and later tackled by several authors (Goedicke, 2003; Goedicke, 2011; Gueli et al., 2010; Jain et al., 2004; Panzeri, 2013; Stella et al., 2013; Zacharias et al., 2002). Many of them noted the problem of age over-estimation being a logical consequence of the analytical technique employed. This is known as a “multigrain aliquot” analysis and it consists in measuring the average luminescence signals emitted by tens or hundreds of grains together. It can only be reliable if all the grains analyzed emit the same amount of luminescence. However, many mortars contain grains that were not sufficiently set to zero by light (optically bleached) during mortar preparation and consequently they emit too high luminescence signals. These signals then pollute an average luminescence signal which explains why in many cases such analyses cannot lead to the correct age determination.

With the aim of suggesting a universal dating procedure that would be applicable on all mortars, involving those affected by insufficient light exposure, we introduced a methodological innovation that consists in the systematic use of the so-called “single grain” OSL technique for dating mortars (SG-OSL; for the technique: (Duller & Murray, 2000); for the application on mortar: (Urbanová & Guibert, 2017)). This approach, which detects the luminescence of each grain individually, is the outcome of recent technological advancements and has become relatively frequent in geological dating applications, but is still rarely employed in mortar dating. Its use on mortars requires some specific considerations arising from the low sensitivity of mortars and their different bleaching mechanism compared to sediments. In addition, compared to the classical “multigrain aliquot” technique, it is a time-consuming analyses requiring specific instrumental equipment. However, it enables to check on bleaching degree and heterogeneity of dated samples by internal control of the method itself and thus ensures more reliable results in the end. In this paper, for the first time we apply the SG-OSL methodology we recently developed (Urbanová & Guibert, 2017) to date mortars of unknown age, fully integrating this approach into archaeological research and thereby demonstrating its far-reaching applicability for historical building studies.

2. Crypt of *Saint Seurin* Basilica in Bordeaux, France

2.1. Historical background

The site of *Saint Seurin* is of particular importance for the paleochristian history of Bordeaux and its transformation from the Late Roman to the medieval urban area. The present church, situated 500 m from ancient Roman fortifications, was erected on a large necropolis whose oldest graves date from the first half of the 4th century AD ((Barraud & Migeon, 2009), p.29). In 1850–54, the remains of a small building were found under the church choir. At the time of this discovery, the remains were interpreted as a small oratory ((Cirot de la Ville, 1840), p.137–138). Within the research on the Christian origins of the city in the 1960s', the remains were believed to be part of the most ancient episcopal complex in Bordeaux ((Maillé, 1960), p.160–165; (Duru, 1982), p.82) and, due to the presence of a large basin, they were attributed to a baptistery. Finally, in the last decade of 20th century, it was understood that the oldest cathedral of Bordeaux must have been located inside the ancient Roman fortifications (Février et al., 1998) and could not therefore be associated with the site of *Saint Seurin*. Nowadays, the ancient construction in the crypt is presumed to have belonged to a primitive mausoleum from Late Roman Antiquity (Barraud & Migeon, 2009; Michel, 2012; Michel et al., 2009) for two reasons: it contains sarcophagi originating from this period and, furthermore, architectural features of the construction are very similar to those of the other mausoleums in the Late Roman Antique necropolis discovered in the south of the present church. However, we do not have any historical source speaking about the function of the ancient building or about its architectural development before 12th century when the present Romanesque church was erected.

2.2. Description of the site

The crypt consists of three parallel naves ended by chapels (Fig. 1a). To simplify the orientation for the reader, we divided the site into three major sectors, A, B and C. In 2006, a visual analysis of the remains in sectors A and B allowed the oldest building phases to be identified (described in detail in (Michel, 2012)). This is summarized below:

1a) The oldest building was orientated on an east-west axis. The remains of the eastern, narrower part of this building can be found in the central chapel (Fig. 1, zone A). It had a rectangular form with a polygonal ending and the ground and the central cavity of this structure were faced with flat squar bricks set in concrete. The perimeter walls, built with small stones and mortar, probably continued towards the west forming a second, larger space which might have belonged to a vestibule (Fig. 1, zone B). Sectors A and B were most likely connected by a small door located in a piece of masonry that separated both spaces. The only remains of this masonry, preserved to the present day, can be seen in Fig. 1e (red circle).

1b-I) Insertion of three sarcophagi A.1, A.2 and A.3 in the central cavity of the oldest building (Fig. 1, zone A).

1b-II) Insertion of eight other sarcophagi B.1–B.8 in the western, wider part of the oldest building (Fig. 1, zone B).

1c) Partial destruction of the original building and **insertion of two more sarcophagi** A.4 and A.5 in its eastern, narrower part in the north-south axis (Fig. 1, violet rectangles). These sarcophagi were excavated in the 19th century and are currently exhibited in the crypt. One of the pits remaining after their excavation is visible in Fig. 1d and f.

2) Covering of all the sarcophagi with a mortar floor. The remains of the mortar floor are visible in different sectors of the crypt.

The main uncertainties linked to the architectural development of the site concern the **dating** of the individual construction phases and

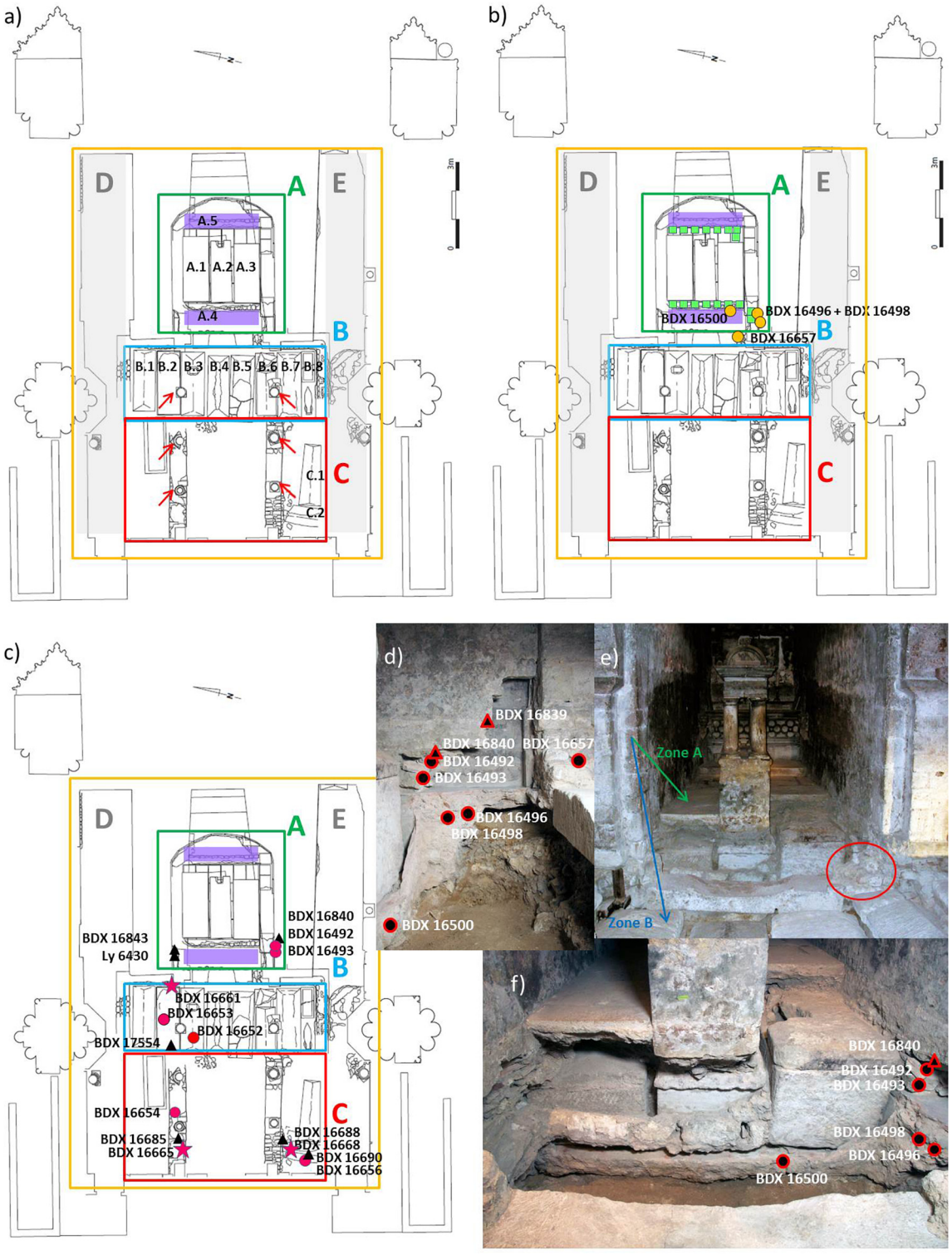


Fig. 1. Plan of the crypt (Barraud & Pichonneau, 1996).
a) The present perimeter of the crypt, composed of three parallel naves, is bordered by the yellow line. The central nave is delimited by six columns marked with red flashes. Zone A, delimited by the green line, corresponds to the chapel of the central nave. It contains the oldest building phase. Zones B and C delimited by the blue and red lines respectively, correspond to two other parts of the central nave as discussed further in the paper. Zones D and E (in grey) represent the lateral naves of the crypt. The elongated violet rectangles show the original position of two decorated marble sarcophagi whose insertion was preceded by a partial destruction of the primitive building (phase 1c).
b) Plan of the crypt and localization of the samples originating from the oldest building. Green rectangles = bricks, yellow circles = mortars
c) Plan of the crypt and localization of the samples taken from the mortar floor covering the sarcophagi: black triangles = dated charcoals, rose circles = dated mortars, rose stars = mortars studied for material characterization (mortar floor).
d, e, and f) Different views on zone A of the crypt and localization of the samples from this sector. (For interpretation of the references to colour in this figure legend, the reader is referred to the web version of this article.)

the **relative chronological classification** of building events between the different sectors of the crypt.

3. Methods and materials

3.1. Dating approaches and sampling

In order to date the oldest construction in the crypt, three laboratories with expertise in thermoluminescence (TL), optically stimulated luminescence (OSL) and archaeomagnetic dating (AM, Sampling report TL_AM 2014) participated in the chronological study of bricks used in the construction of the original building (Guibert et al., 2012; Stella et al., 2014; Bouvier et al., 2015). However, no bricks were used in the subsequent building phases, which is the reason why this approach could not be used to date the reconstructions of the primitive building.

Several years later, new hopes arose with our development of an innovative methodology for mortar dating by SG-OSL. In 2014, a larger excavation and sampling campaign that involved sectors A, B and C was carried out in the crypt (Michel, 2014). The aim of this intervention was to shed light on the construction history of the whole site and to combine archaeological observations with SG-OSL dating of mortars for the first time in an integrated work. When possible, chemical and mineralogical characterization of mortars and radiocarbon dating of charcoals were carried out in order to reinforce archaeological interpretations and dating results. The list of all the samples is presented in Table 1. Their localization can be seen in Fig. 1. The information on the participating laboratories and on the individual dating approaches used in this study is summarized in Table 2.

3.1.1. Details on the SG-OSL dating of mortar samples

The SG-OSL age is calculated as the ratio of the global archaeological dose (corresponding to radioactivity received by the mortar since the construction of the building) to annual dose rate. The mean annual dose was determined by on-site dosimetry (γ and cosmic component of the radioactivity) and by high resolution low back ground gamma spectrometry of natural radio nuclides of the mortar samples (α and β components; (Guibert & Schvoerer, 1991); details also in (Urbanová et al., 2015)). The internal radioactivity of quartz grains used for dating was evaluated by inductively coupled plasma mass spectrometry (ICP-MS). The detailed results of these measurements are included in section C of Supplementary data.

For the determination of the archaeological dose, firstly the luminescence signals emitted by individual quartz grains of the size fraction 200–250 μm extracted from mortars were measured by the single grain technique using TL/OSL DA20 Risø reader with 90Sr/90Y beta source as an irradiation source (dose rate 0.138 ± 0.005 mGy/s on the 1th June 2016). Measurement parameters of the SAR protocol used (Murray & Wintle, 2000) are as follows: preheat 190 °C, cutheat 160 °C, regeneration doses [1.5; 3; 6; 12; 0; 1.5] Gy, test dose 3 Gy, dose recovery 3 Gy. Then, the principal challenge was to identify among the grains emitting the luminescence signals those that were well bleached, i.e. set to zero by light at the moment of mortar making. In order to do so, the obtained experimental distributions of equivalent doses, corresponding to the luminescence signals from individual grains, were submitted to statistical treatment.

To identify the well-bleached grains, two statistical models were used: Internal-external consistency criterion (IEU, (Thomsen et al.,

Table 1
List of all the mortar, brick and charcoal samples discussed in this paper. The brick samples were all taken using a core drill designed for wet cutting with a 25 mm diameter coring auger. The mortars were sampled by using a hammer and a chisel. The mortars dated by SG-OSL are marked in bold.

Sample number	Material	Zone	Origin/localization
Original building			
BDX 13004	Brick	A	
BDX 13006	Brick	A	
TL #4	Brick	A	Bricks used in the construction of the original building
TL# 5	Brick	A	
TL #6	Brick	A	
AM 1- AM 18	18 bricks	A	
BDX 16657-16	**Mortar**	**A-B**	Binding mortar from the masonry separating the zones A and B, associated with the oldest building
BDX 16496	**Mortar**	**A**	
BDX 16498	**Mortar**	**A**	**Foundation mortar of the original building**
BDX 16500	**Mortar**	**A**	
Mortar floor			
BDX 16492-5	**Mortar**	**A**	
BDX 16493-7	**Mortar**	**A**	Mortar associated with covering the sarcophagi A.4 in zone A
BDX 16840-6 (Ly12295)	Charcoal [a]	A	
BDX 16843-16 (Ly12085)	Charcoal	A	
Ly6430	Charcoal	A	
BDX 16652-1	**Mortar**	**B**	
BDX 16653-2	**Mortar**	**B**	**Mortar floor covering the sarcophagi in zone B**
BDX 16661-3	Mortar	B	
BDX 17554 (Ly13127)	Charcoal	B	
BDX 16654-5	**Mortar**	**C**	**Construction mortar from the masonry in zone C**
BDX 16656-15	**Mortar**	**C**	**Mortar floor covering the sarcophagi in zone C**
BDX 16665-8	Mortar	C	Construction mortar from the masonry in zone C
BDX 16668-12	Mortar	**C**	Mortar floor covering the sarcophagi in zone C
BDX 16685-8 (Ly12079)	Charcoal	C	Construction mortar from the masonry in zone C
BDX 16688-12 (Ly12081)	Charcoal	C	Mortar floor covering the sarcophagi in zone C
BDX 16690-15 (Ly12082)	Charcoal [b]	C	Mortar floor covering the sarcophagi in zone C
Stratigraphic levels posterior to the mortar floor			
17552	Charcoal	B	Reconstruction of the column in zone B
16839-2	Charcoal	A	Widening of the wall in zone A

[a] charcoal inside the mortar sample BDX 16492.
[b] charcoal inside the mortar sample BDX 16656.

Table 2
Summary of the physical dating methods used in this study in individual research centers and bibliographic references describing in detail the corresponding measurement protocols.

Sampled material	Laboratory	Dating method	Dated material	Dating protocol/ bibliographic reference
Brick	**IRAMAT-CRPAA** Bordeaux (France)	OSL: Optically stimulated luminescence	QI: Quartz: 80-200 μm	SAR : Murray & Wintle, 2000 and Murray & Olley, 2002
		TL: Thermoluminescence	QI: Quartz: 80-200 μm	TL-AD: Aitken et al., 1964; Blain *et al.*, 2007; Guibert *et al.*, 2009
Brick	**PH3DRA** Catania(Italy)	OSL: Optically stimulated luminescence	QI: Quartz: 90-150 μm	SAR
		OSL: Optically stimulated luminescence	FG: Fine Polymineral: 4-11 μm	FG-SAR: Roberts and Wintle, 2001; Zhang et al., 2007; Kim *et al.*, 2009
		TL: Thermoluminescence	FG: Fine Polymineral: 4-11 μm	TL-AD
Brick	**IRAMAT-CRPAA** Rennes (France)	AM: Archeomagnetism	Magnetic minerals	Lanos, 1998; Lanos *et al.*, 1999; Chauvin *et al.*, 2000; Thellier and Thellier, 1959
Charcoal in mortar	**ArAr** [I] Lyon (France)	C^{14}: Radiocarbon dating	C^{14}	Evin and Oberlin, 1998
Mortar	**IRAMAT-CRPAA** Bordeaux (France)	SG-OSL: Optically stimulated luminescence, single grain technique	QI : Quartz : 200-250 μm	SG-SAR: Duller and Murray, 2000; Thomsen *et al.*, 2005; Urbanová and Guibert, 2017

[I] **Radiocarbon dating of charcoals** was performed by an external analysis in the ^{14}C dating platform ARTEMIS via the *Centre de datation par le radiocarbon Lyon* (CNRS University Lyon 1).

2005; Thomsen et al., 2007)) and 3-parameter minimum age model (MAM-3, (Galbraith et al., 1999)). Both of them require estimating the expected scattering between the well-bleached grains before applying the models.

The ways of estimating such scattering have considerably evolved over recent years. In 2008, many studies systematically included an additional uncertainty of 15% before applying the MAM model to account for the scattering considered typical for well bleached quartz sands (e.g. (Arnold et al., 2008; Demuro et al., 2008; Turney et al., 2008)). In 2012, Thomsen (Thomsen et al., 2012) demonstrated that scattering between the well-zeroed grains depends on individual samples and instead of assuming a constant value, she suggested performing sample-specific laboratory measurements on artificially bleached grains that could be used as input to statistical "age" models. Such measurements allow the estimation of the lowest possible scattering between the well-bleached grains of the given sample.

However, the scattering between the well-bleached grains of natural samples is always higher than the scattering of laboratory bleached samples due to microdosimetric heterogeneity that affects more or less all materials in nature. That is why in 2017 Urbanová and Guibert suggested integrating material characterization of mortars into the dating procedure: a comparative dating study of the known-age mortars (Urbanová & Guibert, 2017) allowed the qualitative classification of samples into three main groups according to their microdosimetric heterogeneity (Table 3). The higher the microdosimetric variations in the sample, the higher the expected scattering between the well-bleached grains, expressed by input σ and a when using MAM and IEU "age" models, respectively.

The age calculation of the poorly bleached mortars discussed in this paper is based on the above mentioned suggestions. First we determine the lowest possible scattering between the well-zeroed grains (sample-specific laboratory measurements). Subsequently, microdosimetric heterogeneity of the samples is qualitatively evaluated by beta imagining and SEM-EDX mapping (Urbanová & Guibert, 2017). Finally, the input parameter to be taken into account for the determination of the global archaeological dose with IEU and MAM models is the mean between the lowest scattering for the given sample and the maximum scattering observed for the given qualitative category.

Unlike previous dating applications, the estimation of the scattering expected between the well-bleached grains is based on detailed material characterization of the studied mortars as the best currently existing solution. This approach arises from a series of experimental observations (Urbanová & Guibert, 2017). The final ages depend on the value of the input used and this is systematically assessed in order to ensure the reliability of the dating results.

Current research efforts aim at developing new statistical models whose use would not require an input parameter to be determined before running the models (Christophe et al., 2018; Guibert et al., 2017)

Table 3
Qualitative classification of mortars according to their microdosimetric heterogeneity based on experimental observations from Urbanová and Guibert (Urbanová & Guibert, 2017).

Category	Main characteristics of mortar	Qualitative evaluation of microdosimetric variations	Input parameter σ/a (expected scattering between well-bleached grains)
1st category	Small grained mortars with low potassium content	Low effect of microdosimetric variations	5–15%
2nd category	Coarse-grained mortars rich in potassium-rich minerals	Microdosimetric variations arise principally from local differences in potassium content	16–25%
3rd category	Coarse-grained mortars rich in zircons, apatites or crushed brick fragments (high content of potassium, thorium and uranium)	Microdosimetric variations arise from local differences in potassium, uranium and thorium content	26–35%*

* In previous study (Urbanová and Guibert, 2017), we detected one exceptional case of mortar that contained large fragments of granite which have much higher radioactivity compared to other rocks. For this sample, the observed over-dispersion arising from microdosimetric heterogeneity was 45%.

Table 4
Dating results obtained for the bricks originating from the oldest building. The TL and OSL dates have already been published separately as central ages at the 68% confidence level (1σ), following convention of luminescence dating, and are thus presented in the same manner. The statistical combination of individual dates using ChronoModel procedure (Lanos and Philippe, 2017; Lanos et al., 2016; Lanos et al., 2015) at 95% confidence level provides the final chronological interval [335, 473] AD with the probability maximum at the year 401 for firing of the bricks.

Laboratory	Brick sample	Dating method	Dated material	Dating protocol	Water content [%]	Annual dose [mGy/year]	Archeo dose [Gy]	Age [years]	Date AD 1σ [years]
IRAMAT-CRPAA	BDX 13004	OSL	QI	SAR	8±3	2.13±0.08	3.42±0.07	1601±72	416±72
Bordeaux (France)	BDX 13006	OSL	QI	SAR	8±3	2.07±0.08	3.38±0.03	1635±70	382±70
(Bouvier et al., 2015)	BDX 13006	TL	QI	AD	8±3	2.23±0.08	3.53±0.49	1584±227	433±227
PH3DRA Catania (Italy) (published in *Stella et al., 2014; open access*)	TL#4	TL	FG	AD		4.27±0.34	6.88±0.51	1610±150	400±150
		OSL	FG	SAR	8±3	2.97±0.24	4.75±0.22	1600±100	410±100
		OSL	QI	SAR		2.13±0.12	3.45±0.14	1620±110	380±110
	TL#5	TL	FG	AD		4.66±0.36	7.82±0.72	1680±180	330±180
		OSL	FG	SAR	8±3	2.94±0.23	4.82±0.19	1640±100	370±100
		OSL	QI	SAR		2.05±0.11	3.30±0.11	1610±100	390±100
	TL#6	TL	FG	AD		5.00±0.45	8.21±0.47	1640±120	370±120
		OSL	FG	SAR	11±4	3.92±0.35	6.32±0.33	1610±110	400±110
		OSL	QI	SAR		3.13±0.20	4.96±0.16	1580±110	430±110
IRAMAT-CRPAA Rennes (France) (details in *Supplementary data, section B*)	Lot of 18 samples	AM	Magnetic minerals	The final chronological interval results from the measurement of the magnetic field of 18 bricks (mean 61.96±1.36 μT reported to Paris).					[318,535]

which would avoid arbitrary classifications of samples into groups. Also, various possibilities of better quantification of microdosimetric heterogeneity are explored (Martin et al., 2015). These researches should contribute to higher accuracy in determining SG-OSL ages in future.

3.2. Physico-chemical characterization of mortar samples

The mortar samples were also studied by means of several analytical methods:

- **optical microscopy:** study of petrography in thin section
- **cathodoluminescence (CL):** evaluating luminescence properties of binder
- **beta autoradiography:** assessing the distribution of beta emissions in mortar matrix
- **laser granulometry:** determining granulometric composition of mortar aggregates
- **scanning electron microscopy coupled with energy dispersed X-ray spectroscopy** (SEM-EDX): chemical composition of homogenized mortar powders and extracted mortar aggregates

The details on equipment and analytical protocols are provided in section A of Supplementary data.

4. Results and discussion

4.1. Origin of the oldest building revealed by a multidisciplinary approach

In Table 4, we sum up all the results obtained by a multimethod dating of bricks originating from the oldest building reported to the calendar year 2017. We note a good convergence of all dating approaches employed. Some of them have been previously published (Stella et al., 2014; Bouvier et al., 2015), others not. The statistical combination of individual dates using ChronoModel procedure (Lanos & Philippe, 2017; Lanos et al., 2015; Lanos et al., 2016) at 95% confidence level provides the final chronological interval [335, 473] AD with the probability maximum at the year 401 AD for firing of the bricks. The apparent homogeneity of the zones where the bricks were sampled and the absence of traces attesting to their re-use indicate that the bricks are on their original placement. If we assume that they were used directly or shortly after their manufacture, we can conclude that the primitive building was erected most probably between the second

Table 5
SG-OSL dating results of mortar samples originating from the oldest building are provided as central ages at the 68% confidence level (1σ), following convention of luminescence dating. Including these results together with the dated bricks into chronological modeling using ChronoModel procedure (Lanos & Philippe, 2017; Lanos et al., 2016; Lanos et al., 2015) at 95% confidence level provides the chronological interval [332,468] AD with probability maximum at the year 400 AD which is in agreement with the initial chronological interval obtained for the firing of the bricks.

Mortar sample	Localisation	Water content[a] [%]	Annual dose [mGy/year]	Archeo dose [Gy]	Nb of grains[b]	σ/a[c] [%]	Age [years]	Date AD 1σ [years]
BDX 16657	Binding mortar from the masonry separating the zones A and B	8 ± 4	1.96 ± 0.08	3.16 ± 0.17	75/113	30	1612 ± 109	406 ± 109
BDX 16500 (published in (Urbanová & Guibert, 2017))	Foundation mortar, floor	8 ± 4	1.68 ± 0.08	2.74 ± 0.13	56/90	30	1631 ± 107	387 ± 107

[a] Water content used for age determination.
[b] Number of grains identified as well-bleached and taken into account for the age calculation/number of grains emitting the luminescence signal.
[c] Expected scattering between the well-bleached grains used for the calculation of archaeological dose: σ (MAM-3)/a (IEU).

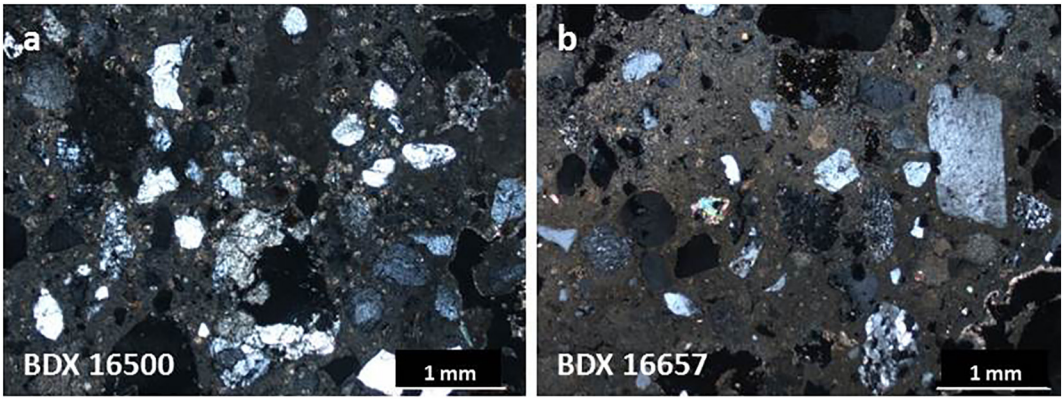


Fig. 2. Thin sections of the mortar samples BDX 16500 (a) and BDX 16657 (b) originating from the oldest building.

half of the 4th and the first half of the 5th century AD.

Dating of bricks provides a *terminus post quem* to the construction of the oldest building. Even if the phenomenon of the re-use of bricks is quite unlikely here, it may be much more problematic in many other cases (e.g. Guibert et al., 2012). We thus integrated **SG-OSL dating of foundation mortar** (BDX 16500) in the study in order to confirm the contemporaneity of brick production with the construction of the oldest building. The mortar BDX 16500 was partially bleached but it contained a predominant proportion of the grains that were well-bleached (set to zero by light) during mortar making. It was also affected by microdosimetric variations arising from the presence of potassium-rich minerals and crushed brick fragments (the third category as described in Section 2.1.1). The dating result 387 ± 107 AD (1σ), which has already been published for methodological purposes ((Urbanová & Guibert, 2017), open access; Table 5), is in agreement with the dating of the bricks.

Another dating result was obtained for the binding mortar BDX 16657 originating from the masonry that separated sectors A and B. According to archaeological interpretations, this masonry also belonged to the primitive building. The sample BDX 16657 showed similar characteristics to BDX 16500 in terms of bleaching degree and microdosimetric heterogeneity. The age determination of BDX 16657 was therefore based on the same assumptions as for the sample BDX 16500 and led to the dating result 406 ± 109 AD (1σ, Table 5) which is in agreement with the date of the construction of the primitive building.

Besides the apparent contemporaneity of the foundations (BDX 16500) and the masonry separating sectors A and B (BDX 16657), petrographic analyses of mortars originating from these constructions reveal the same mineralogical composition (Fig. 2). The aggregates contain monocrystalline phases (quartz, microcline, muscovite) as well as metamorphic rock fragments (quartzite, mica schist) and are rather poorly sorted and sub-angular. Such characteristics of the aggregate clearly distinguish these mortars from the mortars employed in all subsequent building phases that contain almost exclusively well sorted and round quartz grains without any other accompanying minerals (Fig. 3). This observation indicates that the change in raw material sourcing strategies took place between the late antique and early medieval period in the area.

From the methodological point of view, it is also important to mention that two other mortars BDX 16496 and BDX 16498, originating from the

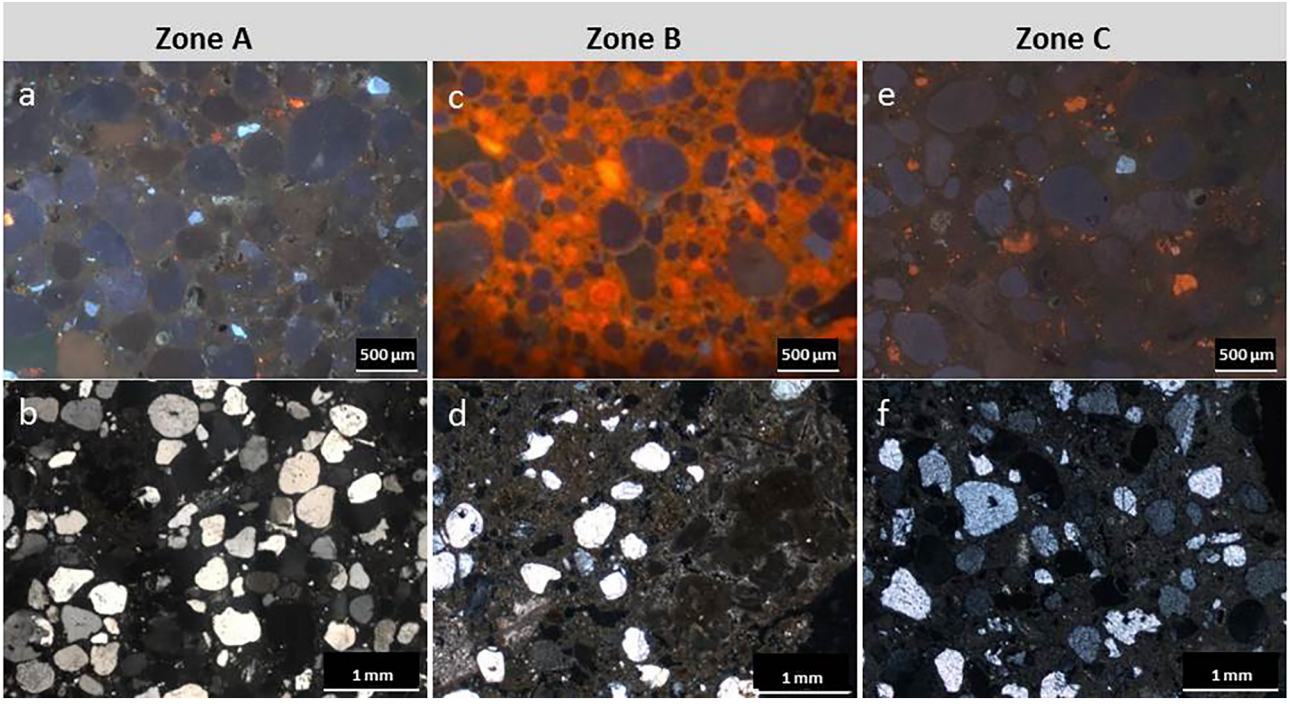


Fig. 3. Cathodoluminescence imaging of studied mortar samples (a, c, e), photos of the thin sections of the same samples in crossed-polarized light (b, d, f).

Table 6
Major components of mortar aggregates extracted from mortars. Analyses by SEM-EDX.

		Weight %							
Zone	Sample	Na_2O	MgO	Al_2O_3	SiO_2	P_2O_5	K_2O	TiO_2	Fe_2O_3
B	BDX 16652-1	1.5	0.4	5.6	88.7	0.2	1.2	0.2	2.2
	BDX 16653-2	0.3	0.3	4.1	92.2	0.1	1.0	0.1	1.9
	BDX 16661-3	0.7	0.4	4.4	91.4	0.2	0.8	0.2	1.9
A	BDX 16492	0.2	0.1	2.5	95.5	0.1	0.7	0.1	0.8
	BDX 16493	0.3	0.1	2.4	95.4	0.2	0.7	0.2	0.7
C	BDX 16654-5	1.3	0.2	3.6	92.6	0.1	0.7	0.2	1.3
	BDX 16665-8	0.3	0.2	3.5	93.8	0.1	0.7	0.2	1.2
	BDX 16668-12	0.4	0.3	4.3	92.1	0.2	0.9	0.2	1.6
	BDX 16656-15	0.7	0.3	4.3	91.7	0.2	0.9	0.2	1.7

same construction phase but located higher in the perimeter wall, were extremely poorly bleached and did not contain sufficient number of grains set to zero by light during mortar making. Very interesting observations can be made if we compare the microstructure of these mortars. While BDX 16500, a foundation mortar that was well-bleached, shows characteristics of a careful fabrication procedure (well sorted, well mixed, hydraulic), BDX 16496 and BDX 16498 contain poorly sorted, coarse aggregate and numerous lime lumps linked to insufficient slaking (imperfections in the preparation procedure). An intentional differentiation in the preparation technology within the same construction phase is thus observed and this may also explain the differences in the degree of bleaching. We can raise the hypothesis that well-worked mortar mixtures require a longer preparation procedure which increases the probability of exposure of quartz grains in mortar to light and consequently leads to a better degree of bleaching in such samples.

4.2. Classification of building phases via mortar dating and analyses

4.2.1. Burying the sarcophagi: one single or several building phases?

4.2.1.1. Typochronological dating of the sarcophagi. As already mentioned, several sarcophagi are placed in the crypt. Their position can be seen in Fig. 1. The features of the three limestone sarcophagi A.1, A.2 and A.3 from zone A and of the eight calcite and marble sarcophagi B.1-B.8 in zone B, all orientated east-west, allow typochronological dating between the 4th and the 5th centuries AD (Rougé et al., 2015). Stylistic analyses of two amply decorated marble sarcophagi A.4 and A.5 from zone A orientated in the north-south direction (violet rectangles in Fig. 1), whose insertion was preceded by partial destruction of the primitive building, indicate the date of their fabrication between the end of the 4th and the end of the 5th century AD (Cazes, 2006). Finally, the features of two sarcophagi of trapezoidal form C.1 and C.2 in zone C correspond to the pattern that first appeared in the Aquitane region between the 6th century and the beginning of the 8th century AD (Rougé et al., 2015). Sarcophagi C.1 and C.2 are thus most likely younger than those in the zones A and B.

However, traditions in manufacturing sarcophagi were evolving progressively and the patterns appearing in the 6th century AD might have existed parallel to the older ones, whose use was gradually fading out. In addition, it is not known either when the sarcophagi were inserted in the masonry, or if their original location corresponds to their present position. For all these reasons, dating of the sarcophagi has limited potential for understanding the construction history of the crypt. Besides other things, this explains why we were searching for new dating strategies. Nevertheless, the typo-chronology of the sarcophagi can be used as stratigraphic constraint when constructing chronological sequences; in this context, their dating gives *terminus post quem* to the stratigraphic levels that cover them.

4.2.1.2. Archaeological questions about the construction history. A stratigraphic level of particular importance is the mortar floor covering all the sarcophagi. It represents a stage of important restructuring of the monument and probably indicates the end of its funerary function. In 2012 (Michel, 2012), this transformation was considered as one single building phase. During the archaeological excavations in 2014 (Michel, 2014), it appeared that the situation is much more complicated.

One of the most important questions concerns the interface between zones B and C. In lower altitudes corresponding to the most ancient levels, we clearly identified dissimilarities in stratigraphy which would indicate that the architectural development of zone C was independent of zone B. Two fragments of masonry, one in the northern and one in the southern part of the crypt at the limit of zones B and C were discovered. They most probably correspond to the remains of the wall delimiting zones B and C in the past. However, archaeologically it is difficult to establish which part developed first.

The link between zones A and B is also more complicated than initially believed since a physical relationship between these sectors was interrupted during the 19th century excavations. In particular, archaeology does not enable us to understand when the two marble sarcophagi A.4 and A.5 were inserted and if they were buried at the same time as sarcophagi B.1 and B.8. In order to shed light on incoherencies in stratigraphy and to establish the chronology of the site, dating and characterization of the mortar floor covering the sarcophagi were carried out.

4.2.1.3. Material characterization of the mortar floor covering the sarcophagi. Mortars discussed in this part originate from the mortar floor in sectors A, B and C, as listed in Table 1 and shown in Fig. 1c. According to the petrographic study, all the samples contain predominant proportion of isolated quartz grains of a rounded form, followed by very small quantities of feldspars and traces of micas, silex and metamorphic rock fragments. SEM-EDX analyses revealed that SiO_2 content in mortar aggregates is 88–96% (Table 6).

Table 7
Major components of mortar powder pellets. Analyses by SEM-EDX.

		Weight %								
Zone	Sample	Na_2O	MgO	Al_2O_3	SiO_2	P_2O_5	K_2O	CaO	TiO_2	Fe_2O_3
B	BDX 16652-1	0.4	0.8	5.9	46.4	0.1	1.0	42.6	0.4	2.4
	BDX 16653-2	0.2	0.7	5.6	47.9	0.0	1.0	41.9	0.4	2.3
	BDX 16661-3	0.3	0.7	4.9	48.8	0.0	0.9	41.9	0.3	2.2
A	BDX 16492	0.2	0.3	3.3	72.0	0.2	1.0	21.6	0.3	1.1
	BDX 16493	0.2	0.3	3.0	68.2	0.1	0.9	26.1	0.1	1.1
C	BDX 16654-5	0.3	0.8	5.2	53.0	0.2	1.1	37.3	0.2	1.9
	BDX 16665-8	0.4	1.1	6.9	53.2	0.1	1.4	34.2	0.4	2.3
	BDX 16668-12	0.9	0.9	6.1	59.2	0.3	1.5	28.6	0.2	2.3
	BDX 16656-15	0.5	0.8	5.7	58.6	0.2	1.3	30.6	0.1	2.2

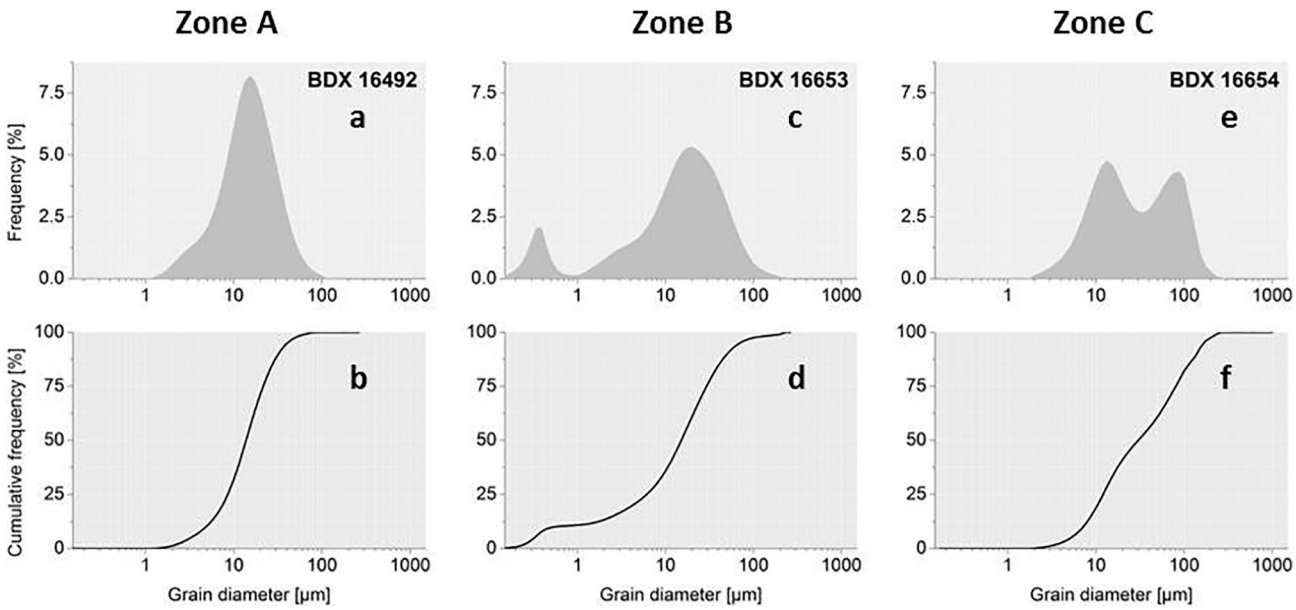


Fig. 4. Granulometic distributions of silts extracted from the studied mortar samples (a, c, e) and corresponding cumulative curves (b, d, f).

Such a high content of silica does not allow the classification of mortars into groups according to their chemical composition. The mineralogical composition of aggregates is very similar which probably indicates that the raw material is of the same or very similar provenance. Nevertheless, apparent differences are observed in recipes used for the preparation of mortars which allows us to distinguish three groups. The ratio of binder to aggregate based on the results of SEM-EDX powder pellets (Table 7) is equal approximately to 1:3 for the mortar floor in zone A, to 2:3 for zone B and to 1:2 for zone C. The mortar floor in zones B and C contains many limestone fragments and is richer in Al and Fe (attributed to clay minerals) than in zone A.

Even more significant differences were observed with cathodoluminescence imaging. The mortar floor in zone A is characterized by brown to grey luminescence of the binder, whereas the binder of the mortar floor in zone B shows bright red-orange luminescence and the one from zone C shows brown to dark red luminescence (Fig. 3). The mortar aggregates from individual zones reveal very different granulometic profiles which can be seen when comparing the granulometric curves of silts extracted from the studied samples (Fig. 4). All above mentioned observations indicate that the mortar floor directly covering the different sarcophagi in zones A, B and C does not originate from the same preparation procedure. Therefore, we assume that the sarcophagi might have been buried in three building stages.

4.2.1.4. SG-OSL dating of the mortar floor covering the sarcophagi. The SG-OSL measurements of quartz grains extracted from selected mortars showed **heterogeneous bleaching** which causes scattering in the equivalent dose distributions of individual samples. Such results clearly demonstrate the necessity of analyzing each single grain of quartz separately to obtain exploitable dating results. The presence of the well-zeroed grains (whose bleaching occurred at the moment of mortar making) is demonstrated by high frequency peaks visible at the lowest dose region of the corresponding histograms (Fig. 5).

The majority of the samples are characterized by low average content of potassium oxide K_2O (0.5–1.3%). The mortars are rather small-grained and only sporadically contain minerals rich in potassium. Also, according to the SEM-EDX analyses they do not contain any apatites and zircons whose presence might contribute to microdosimetric variations. Finally, the results of beta imaging do not indicate significant heterogeneity of beta emissions in the mortars studied (Fig. 6a, c). All these analyses lead us to conclude that the samples originating from the mortar floor are **not affected by significant microdosimetric variations**, contrary to the foundation mortar of the primitive building (Fig. 6e). The samples from the mortar floor thus belong to the first category as defined in Section 3.1.1 (Table 3). Hence, heterogeneous bleaching is considered as the principal extrinsic source of scattering in measured equivalent dose distributions.

The archaeological doses were calculated as explained in Section 3.1.1. Both statistical models used for the calculation of archaeological dose, MAM-3 and IEU, give coherent results, except for the mortar BDX 16653. Due to poor bleaching of this sample, only a few grains were identified as bleached by MAM-3. In consequence, there is a good deal of uncertainty about dating result. The number of grains taken into account is systematically lower when using MAM-3 than IEU and final dating results from MAM-3 are associated with higher uncertainty.

Table 8 sums up all data used for the final age calculation. If we summarize the results of SG-OSL dating, sarcophagi B.1–B.8 (zone B) were buried between the 5th and 6th centuries AD, sarcophagi A.4 and A.5 between the end of the 6th and the beginning of the 8th centuries AD and sarcophagi C.1 and C.2 between the 9th and the 11th centuries AD.

4.2.1.5. Radiocarbon dating of charcoals found in the mortar floor. Numerous charcoal fragments were found in the mortar floor. Two of them were directly embodied within the mortar samples used for SG-OSL dating which allowed the comparison of both methods. The results obtained for the charcoals are presented in Table 8. They show good agreement between radiocarbon dating of charcoals and SG-OSL dating of mortars originating from the same stratigraphic levels. However, we must keep in mind a potential risk of an “over-ageing effect” when dating the charcoal from mortar (e.g. (Heinemeier et al., 2010; Tubbs & Kinder, 1990)) as the date reflects the moment of the growth of vegetal cells; that gives a *terminus post quem* to the construction. Agreement obtained in this particular case cannot therefore be taken as a general rule and one must always be cautious when interpreting charcoal dating in the context of building archaeology. By contrast, contemporaneity of the mortar bleaching with the building process is indubitable.

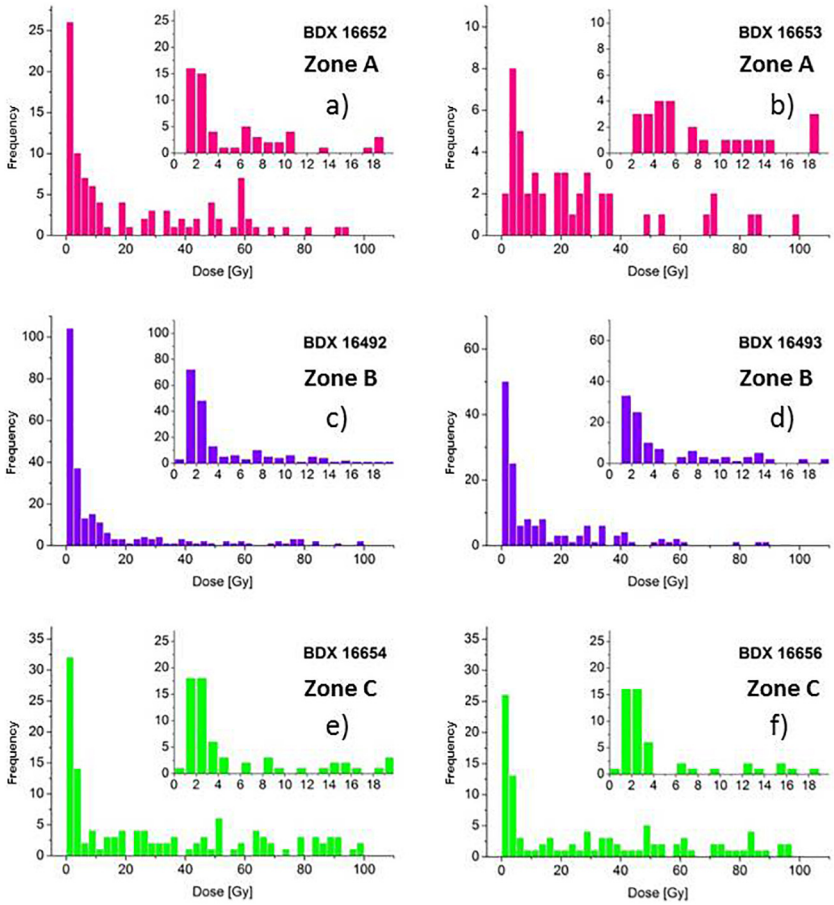


Fig. 5. Distributions of equivalent doses for the individual quartz grains extracted from the mortars and measured by SG-OSL.

4.2.1.6. Chronological reconstruction and archaeological interpretations. A statistical combination of all dating results obtained was performed by means of the ChronoModel procedure (Lanos & Philippe, 2017; Lanos et al., 2015; Lanos et al., 2016) at 95% confidence level. The chronological modeling, that was carried out independently for each of the zones A, B and C, is based on the concept of event date determined by calendar dates that are assumed contemporary. For each event date, we assumed a priori a uniform distribution in the "study period", which is set by the interval [−500, 1800] on the basis of the chronological context of the site. The dating results obtained for mortars and charcoals originating from the same stratigraphic levels were supposed to be contemporaneous and therefore were combined in the modeling in order to date the same event. In case there are preserved stratigraphic relationships between two stratigraphic levels, the events corresponding to these levels were linked by temporal order relationships, assuming the upper stratigraphic layers to be younger. Stratigraphic constraints, expressed with the arrows pointing at stratigraphically younger layers, contribute to more accurate results of the modeling.

Fig. 7a shows the construction of the chronological model for zone A. We distinguish three different events with which individual SG-OSL, OSL, TL, archaeomagnetic and radiocarbon dating results are associated. Information on typochronological dating of the sarcophagi and on the construction of the Romanesque church was introduced in the modeling as chronological "bounds", i.e. TPQ and TAQ, respectively. For example, if sarcophagi A.4–A.5 were produced between 400 and 500 AD, they could not have been buried before 400 AD. So, the TPQ to the event "covering sarcophagi A.4–A.5" is 400 AD. Since the date of this TPQ was introduced in the model as a "bound", it represents a fixed value that will not be influenced by the modeling itself towards an earlier or a later date (contrary to the "event"). However, this TPQ will play an important role as a stratigraphic constraint to the event "covering sarcophagi A.4–A.5".

The bound corresponding to the "typochronology of sarcophagi A.4–A.5" is considered to be independent of the event "construction of the primitive building". This is why they are not connected with an arrow. However, both of them are linked by temporal order relationships with the event "covering the sarcophagi A.4–A.5", and therefore connected by the arrows.

Fig. 7b shows the results of the modeling for zone A: final calendar dates determining each event date were expressed as marginal posterior probability distributions resulting from the statistical combination of individual dating results shown in Fig. 7a. The same procedures were applied to run the chronological modeling for zones B and C as demonstrated in Figs. 8 and 9, respectively. We observe good agreement between the individual dating results within each building event.

Concerning the results of the modeling, particular attention should be paid to violet probability distributions. They indicate that the covering of the sarcophagi in sectors A and B was not contemporary. Sarcophagi B.1–B.8 were buried between [384, 632] AD with probability maximum at 501 AD, while sarcophagi A.4–A.5 were buried between [582, 778] AD with probability maximum at 683 AD. It can be noted that the chronological intervals obtained partly overlap. The limits of the dating approaches employed do not allow chronological separation of these two events. Nevertheless, archaeological observations of stratigraphy as well as considerable differences revealed by characterization between the mortars from these two sectors rather reinforce the hypothesis of two different building stages.

All these observations differ from the preceding theory that the

Table 8
Dating results for the mortars and the charcoals originating from the different sectors of the crypt. The SG-OSL dates are usually presented as central ages at the 68% confidence level (1σ), following convention of luminescence dating. However, in order to enable an easier comparison between the SG-OSL and the C^{14} dates, we also present these results at the 95% confidence level (2σ). Final chronological modeling allows both SG-OSL and radiocarbon dates to be combined at 95% confidence level (2σ).

Mortars : SG-OSL ages/dates											
Zone	Mortar sample	Water content [I] [%]	Age model	OD_{min} [II] [%]	σ/a [III] [%]	Archeo dose [Gy]	Nb of grains [IV]	Annual dose [mGy/year]	Age [years]	Date AD 1σ [years]	Date AD 2σ [years]
B	BDX 16652-1	7.0±3.5	MAM-3	8	11	1.94±0.07	30/96	1.29±0.07	1505±99	513±99	513±138
			IEU			1.95±0.05	46/96		1513±92	505±92	505±128
	BDX 16653-2	7.0±3.5	MAM-3	11	13	3.77±0.50	4/58	2.20±0.10	1711±239	307±239	307±334
			IEU			3.53±0.24	12/58		1602±130	416±130	416±187
A	BDX 16492-5	7.0±3.5	MAM-3	9	12	1.69±0.05	89/240	1.24±0.06	1357±75	661±75	661±104
			IEU			1.69±0.04	90/240		1357±71	661±71	661±99
	BDX 16493-7	7.0±3.5	MAM-3	8	12	1.72±0.08	35/145	1.21±0.05	1364±70	654±70	654±97
			IEU 8			1.73±0.05	50/145		1364±66	654±66	654±92
C	BDX 16654-5	7.0±3.5	MAM-3	7	11	1.44±0.14	10/129	1.34±0.06	1071±115	947±115	947±160
			IEU			1.48±0.06	22/129		1101±68	917±68	917±95
	BDX 16656-15	7.0±3.5	MAM-3	8	11	1.55±0.20	11/108	1.52±0.07	1022±140	996±140	996±195
			IEU			1.54±0.08	19/108		1015±70	1003±70	1003±97

Charcoals from the mortar floor : C^{14} ages/dates			
Zone	Charcoal sample	C^{14} age (yr BP)	C^{14} cal. age AD [VI]
B	BDX 17554	1625±30	353-537
A	BDX 16840-6 (inside the mortar BDX 16492)	1285±30	666-771
	BDX 16843-16	1345±30	641-765
	Ly6430	1280±30	665-777
C	BDX 16690-15 (inside the mortar BDX 16656)	1150±30	776-971
	BDX 16688-12	1200±30	715-940
	BDX 16685-8	1160±30	773-968
Charcoals from the stratigraphic levels posterior to the mortar floor : C^{14} ages/dates			
B	BDX 17552	1175±30	770-963
A	BDX 16839	1145±30	776-975

[I] Water content used for age determination.
[II] The lowest possible scattering between the well-bleached grains (determined by samples specific laboratory measurements on artificially bleached grains).
[III] Expected scattering between the well-bleached grains used for the calculation of archaeological dose: σ (MAM-3)/a (IEU).
[IV] Number of grains identified as well-bleached and taken into account for the age calculation/number of grains emitting the luminescence signal.
[V] Dating of samples BDX 16492 and BDX 16493 has already been published in Urbanová and Guibert (Urbanová & Guibert, 2017). In the meanwhile, more precise measurements of radioactivity were performed on the higher number of quartz grains which allowed more precision for previously published dates.
[VI] Calibration curve used (Reimer et al., 2013).

sarcophagi from zones A and B were buried at the same time. As explained in Section 4.1, the original Late Roman Antiquity building was divided into two rooms by masonry standing between zones A and B. Only a small entrance whose doorstone is still visible (Fig. 1e) connected both areas. However, since that masonry does not exist anymore, current configuration of the space makes us perceive zones A and B as a single space which might have influenced the previous interpretations.

In zone C, the mortar floor covering sarcophagus C.2 in the southwestern part of the sector was dated between [804, 1020] AD with probability maximum 917 AD. The construction mortar from the northwestern part of this sector indicates the same chronological interval. In addition, the material characterization of the mortars from this sector shows identical mineralogical and chemical composition, very different from those in sector B. It can thus be concluded that the building remains studied and dated in zone C belong to a later construction than those in sectors A and B.

Finally, we can also note that the dating of the building remains in zone C reveals the same chronology as two charcoals taken in the levels posterior to covering the sarcophagi in sectors A and B. The layers where these charcoals were taken are associated with a reconstruction taking place after the covering the sarcophagi. However, due the lack of direct stratigraphic relationships between the sectors A, B and C, it is not currently possible to prove that all these dates correspond to the same building event. The future research, consisting in the finer stratigraphic analyses of the elevated parts of the masonries and new dating analyses will shed light on these questions. It is possible that in the period between the 9th and 11th centuries AD, a larger reconstruction that resulted in the first unification of the sectors A, B and C within the same building was undertaken.

5. Conclusions

The aim of the present paper is to familiarize the scientific community with the new possibilities that SG-OSL dating of mortar offers to building archaeology and to underline the importance of close interdisciplinary collaboration for the studies of historical monuments. We focused on the Early Middle Ages as one of the most problematic

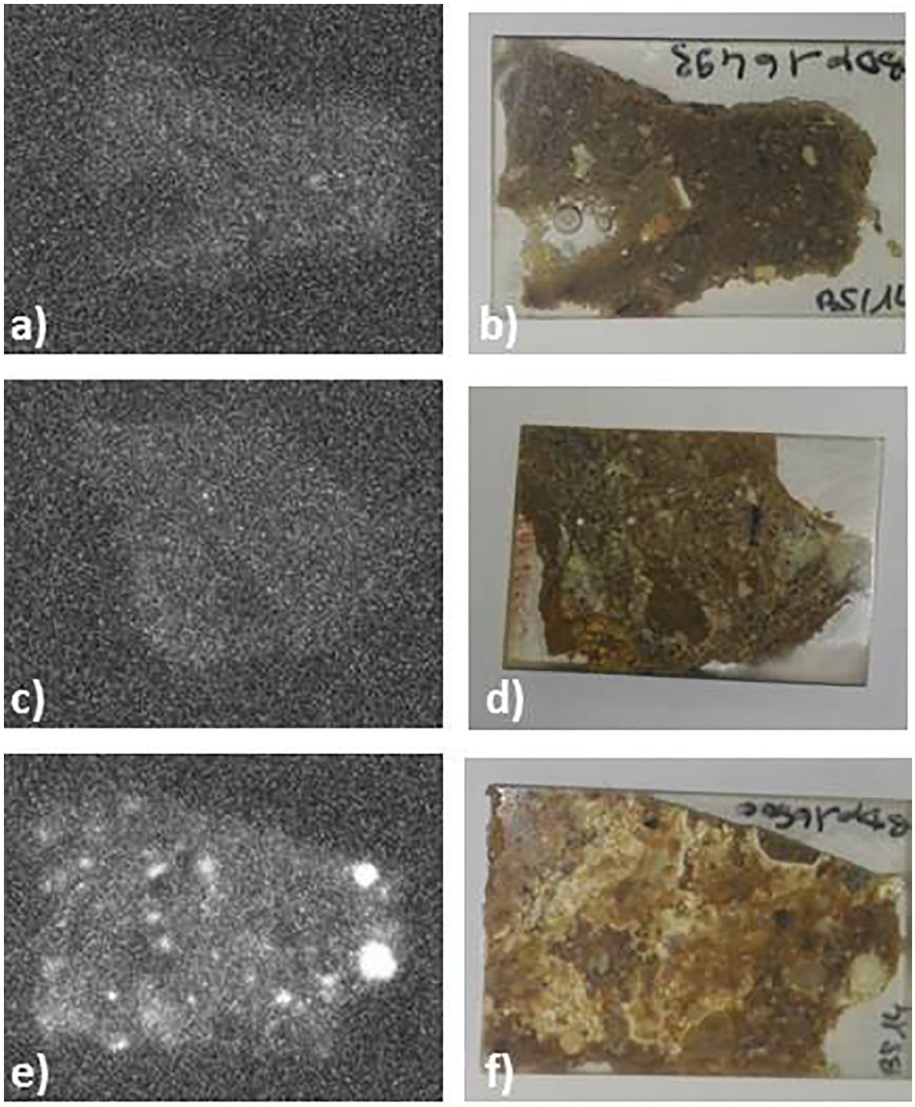


Fig. 6. Images obtained by beta autoradiography (a, c, e) and corresponding macrophotographs (b, d, f). The first (a,b) and the second (c,d) mortar sample originate from the level corresponding to covering the sarcophagi in zone A and B respectively, while the third sample (e,f) represents the foundation mortar of the primitive building. Beta radioactive emissions are more homogeneous for samples BDX 16493 (a, b) and BDX 16653 (c, d) than for sample BDX 16500 (e, f).

periods when it comes to understanding the stratigraphy and chronology of ancient buildings. However, the research presented here has far-reaching applicability in the archaeology of buildings and can be applied for all historical periods when mortar was used as building material.

The methodology is demonstrated by the complex case study of the crypt of Saint Seurin Basilica in Bordeaux. Basically, the results acquired can be divided into two phases. The first stage was focused on the multimethod chronological study of bricks. It allowed the construction of the oldest building in the crypt to be dated to, most probably, between the second half of the 4th century and the first half of the 5th century AD. The SG-OSL dating of mortars originating from this building phase led to the same results; that was particularly encouraging for the study of subsequent building phases where mortar analysis represented the only possibility of dating.

The second stage was focused on the clarification of a chronological hiatus in the history of the site in the period between the 5th century and the end of 11th centuries AD. Up to now, no source of information allowed better understanding of reconstructions that took place in the crypt in the past. Thanks to the combination of SG-OSL dating of mortars with stratigraphic analyses, mortar characterization and radiocarbon dating of charcoals, we distinguished at least three chronologically distinct building phases that came after the erection of the Late Roman Antiquity structure. Thus we identified the traces of progressive transformations and extensions of the oldest building. The study allows us to conclude that the present perimeter of the crypt does not reflect the layout from the 9th century AD as initially believed, but it is the result of the reconstruction processes running through multiple stages between the 5th and the 11th centuries AD. This is an essential element of knowledge for the history of the crypt for which no written sources exist before the 13th century AD. It demonstrates that the site of Saint Seurin has been continuously occupied since the Late Roman Antiquity, reflecting a cultural and symbolic value that has persisted for more than 1500 years. Even if it might seem obvious, we feel it is



Fig. 7. Procedure and results of the statistical combination (95% confidence level) of all the dating results obtained for the samples originating from zone A.

important to underline that we avoid any historical prejudice when reconstructing the construction history of the monument; our conclusions are based on thorough observations in situ, as well as analyses and dating of building materials. The possibility of dating mortar whose production is contemporary to the moment of construction raises hopes of deepening knowledge about many currently poorly known, fragmentary or partly rebuilt ancient buildings.

It is logical that the construction of chronological sequences can only be successful if stratigraphic analyses by experienced archaeologist are part of the dating process. However, the results of material characterization and dating help archaeologists to progress in their understanding of a site by revealing new possible interpretations that do not



Fig. 8. Procedure and results of the statistical combination (95% confidence level) of all the dating results obtained for the samples originating from zone B.

necessarily follow usual patterns. That is why we feel it is essential to point out that the results of this work arise from continuous and reciprocal interaction between archaeologists and dating specialists. Especially in case of fragmentary ancient monuments unknown by written sources and affected by reconstructions or past excavations, a constructive and convincing archaeological interpretation can only be reached if all scientific disciplines are truly combined together as we have done in this study.

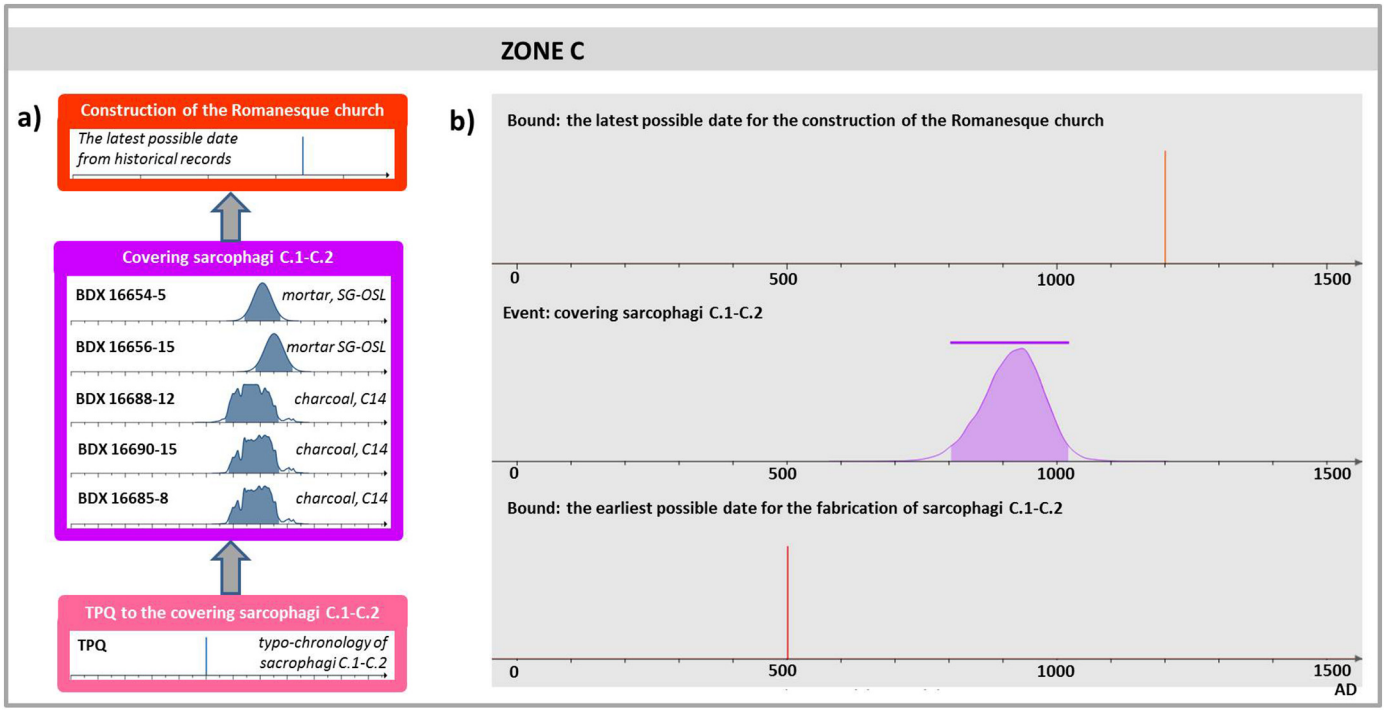


Fig. 9. Procedure and results of the statistical combination (95% confidence level) of all the dating results obtained for the samples originating from zone C.

Acknowledgements

We are grateful to the following organizations which have supported this research financially: CNRS-INSHS [French National Center for Scientific Research - Institute of Human and Social Sciences], Regional Council of Aquitane [equipment, research grant], University Bordeaux-Montaigne [PhD grant and special support for research programs], Bordeaux City Hall. This project was co-financed by the labex LaScArBx [Bordeaux Archaeological Sciences Labex] administrated by ANR [*Agence Nationale de la Recherche*] with the reference ANR-10-LABX-52. A part of this research was carried out within the framework of the European research group (GdRE) *Ceramic Building Materials and New Dating Methods (CNRS n° 227; 2005 – 2012; (Guibert et al., 2012))*.

We would also like to express our thanks to the following institutions for the sampling authorization: Bordeaux City Hall, Regional Service of Archaeology *Nouvelle Aquitaine* (DRAC-SRA). Special thanks to Yannick Lefrais (SEM-EDX), Brigitte Spiteri (preparation of thin sections), Jean-Baptist Javel (field work and preparation of thin sections), Alain Quefellec (granulometric analyses). Finally, we would like to thank the reviewers for constructive suggestions provided during the revision process of this manuscript.

Appendix A. Supplementary data

Supplementary data to this article can be found online at https://doi.org/10.1016/j.jasrep.2018.04.009.

References

Aitken, M.J., Tite, M.S., Reid, J., 1964. Thermoluminescence dating of ancient ceramics. Nature 202, 1032–1033.

Arnold, L.J., Roberts, R.G., MacPhee, R.D.E., Willerslev, E., Tikhonov, A.N., Brock, F., 2008. Optically dating of perennially frozen deposits associated with preserved ancient plant and animal DNS in north-central Siberia. Quat. Geochronol. 3, 114–136.

Barraud, D., Migeon, W., 2009. Topographie chrétienne de Bordeaux dans l'Antiquité tardive à la lumière des nouvelles découvertes archéologiques. In: Cartron, I., Barraud, D., Henriet, P., Michel, A. (Eds.), Autour de Saint-Seurin: Lieu, Mémoire, Pouvoir, des Premiers Temps Chrétiens à la fin du Moyen Âge, Actes de colloque de Bordeaux 12–14/10/2009, Bordeaux, pp. 23–33 (351 p., Ausonius editions, ISBN: 978-2-35613-012-2–9).

Barraud, D., Pichonneau, J.-Fr, 1996. Bordeaux, Saint-Seurin. Bilan scientifique de la recherche archéologique en Aquitaine, 1996. DRAC Aquitaine 55–59.

Blain, S., Guibert, P., Bouvier, A., Vieillevigne, E., Bechtel, F., Sapin, C., Baylé, M., 2007. TL-dating applied to building archaeology: the case of the medieval church Notre-Dame-sous-Terre (Mont-Saint-Michel, France). Radiat. Meas. 42, 1483–1491.

Bøtter-Jensen, L., Solongo, S., Murray, A.S., Banerjee, D., Jungner, H., 2000. Using OSL single-aliquot regenerative-dose protocol with quartz extracted from building materials in retrospective dosimetry. Radiat. Meas. 32 (5–6), 841–845.

Bouvier, A., Sapin, C., Guibert, P., Blain, S., 2015. Les apports de la chronologie par luminescence: étude de la crypte de la collégiale Saint-Seurin de Bordeaux. In: Actes du colloque de l'Association Française d'Archéologie Mérovingienne, Bordeaux octobre 2009, Aquitania. suppl. 34. pp. 469–478.

Büttner, S., 2014. L'analyse des liants de maçonnerie et son apport à la compréhension chronologique et technique de la construction. In: Bolle, C., Coura, C., Léotard, J.M. (Eds.), L'archéologie des Bâtiments en Question. Un Outil Pour les Connaitre, les Conserver et les Restaurer, Actes du Colloque International, Liège, 9–10/11/2010, Namur (Études et Documents, Archéologie, 35), pp. 103–114 (390p).

Carò, F., Riccardi, M.P., Mazzilli Savini, M.T., 2008. Characterization of plasters and mortars as a tool in archaeological studies: the case of Lardirago castle in Pavia, Northern Italy. Archaeometry 50, 85–100.

Cazes, D., 2006. Les sarcophages paléochrétiens sculptés en marbre de Toulouse et la nécropole de Saint Sernin. In: Sapin, C. (Ed.), Stucs et décors de la fin de l'Antiquité au Myen âge (V^{e}-XII^{e} siècle), Proceedings of International Conference, Poitiers, 16–19/9/2004. Brepols Publishers (ISBN 978-2-503-52515-0).

Chauvin, A., Garcia, Y., Lanos, P., Laubenheimer, F., 2000. Paleointensity of the geomagnetic field recovered on archaeomagnetic sites from France. Phys. Earth Planet. Inter. 120, 111–136.

Chiarelli, N., Miriello, D., Bianchi, G., Fichera, G., Giamello, M., Turbanti Memmia, I., 2015. Characterisation of ancient mortars from the S. Niccolò archaeological complex in Montieri (Tuscany - Italy). Constr. Build. Mater. 96, 442–460.

Christophe, C., Philippe, A.A., Guérin, G., Mercier, N., Guibert, P., 2018. Bayesian approach to OSL dating of poorly bleached sediment samples: Mixture Distribution Models for Dose (MD2). Radiat. Meas. 108, 59–73. http://dx.doi.org/10.1016/j.radmeas.2017.10.007.

Cirot de la Ville, J.-P.-A., 1840. Notice sur l'église Saint-Seurin de Bordeaux, Bordeaux.

De Luca, R., Cau Ontiveros, M.A., Miriello, D., Pecci, A., Le Pera, E., 2013. Archaeometric study of mortars and plasters from the Roman City of Pollentia (Mallorca-Balearic Islands). Periodico di Mineralogia 82 (3), 353–379.

Demuro, M., Roberts, R.G., Froese, D.G., Arnold, L.J., Brock, F., Bronk Ramsey, C., 2008. Optically stimulated luminescence dating of single and multiple grains of quartz from perennially frozen loess in western Yukon Territory, Canada: comparison with radiocarbon chronologies for the Late Pleistocene Dawson tephra. Quat. Geochronol. 3, 346–364.

Duller, G., Murray, A.S., 2000. Luminescence dating of sediments using individual mineral grains. Andean Geol. 5, 87–106.
Duru, R., 1982. La crypte de l'église Saint-Seurin de Bordeaux, en Hommage à la Mémoire de la Marquise de Maillé. Sauvegarde de l'art Français. vol. 2. pp. 57–89.
Evin, J., Oberlin, C., 1998. La méthode de datation par le radiocarbone. In: Ferdière, A. (Ed.), Les Méthodes de Datation en Laboratoire, pp. 75–118 (Collection « Archéologiques », Edition Errance, Paris).
Février, P.-A., Barraud, D., Maurin, L., 1998. "Bordeaux", Topographie chrétienne des cités de la Gaule des origines au milieu du VIIIe siècle, t. X., Province ecclésiastique de Bordeaux (Aquitania Secunda), Paris. pp. 18–33.
Frizot, M., 1975. Mortiers et enduits peints antiques. Université Dijon, Etude technique et archéologique. Centre des recherches sur les techniques gréco-romains.
Furlan, V., Bissenger, P., 1975. Les mortiers anciens, histoire et essais d'analyse scientifique. In: Revue Suisse d'Art et d'Archéologie, pp. 166–178.
Galbraith, R.F., Roberts, R.G., Laslett, G.M., Yoshida, H., Olley, J.M., 1999. Optical dating of single and multiple grains of quartz from Jinmium Rock Shelter, Northern Australia: part I, experimental design and statistical models. Archaeometry 41 (2), 339–364. http://dx.doi.org/10.1111/j.1475-4754.1999.tb00987.x.
Goedicke, C., 2003. Dating historical calcite mortar by blue OSL: results from known age samples. Radiat. Meas. 37, 409–415.
Goedicke, C., 2011. Dating mortar by optically stimulated luminescence: a feasibility study. Geochronometria 38 (1), 42–49.
Gueli, A.M., Stella, G., Troja, S.O., Burrafato, G., Fontana, D., Ristuccia, G.M., Zuccarello, A.R., 2010. Historical buildings: Luminescence dating of fine grains from bricks and mortar. In: Il Nuovo Cimento 125 B.
Guibert, P., Schvoerer, M., 1991. TL-dating: low background gamma spectrometry as a tool for the determination of the annual dose. Nucl. Tracks Radiat. Meas. 18 (1–2), 231–238. http://dx.doi.org/10.1016/1359-0189(91)90117-Z.
Guibert, P., Bailiff, I.K., Blain, S., Gueli, A.M., Martini, M., Sibilia, E., Stella, G., Troja, S., 2009. Luminescence dating of architectural ceramics from an early medieval abbey: the St-Philbert intercomparison (Loire Atlantique, France). Radiat. Meas. 44, 488–493.
Guibert, P., Bailiff, I., Baylé, M., Blain, S., Bouvier, A., Büttner, S., Chauvin, A., Dufresne, P., Gueli, A., Lanos, P., Martini, M., Prigent, D., Sapin, C., Sibilia, E., Stella, G., Troja, O., 2012. The use of dating methods for the study of building materials and constructions: state of the art and current challenges. In: Proceedings of the 4th Congress on Construction History Paris 3–7 July 2012, pp. 469–480.
Guibert, P., Christophe, C., Urbanová, P., Guérin, G., Blain, S., 2017. Modeling incomplete and heterogeneous bleaching of mobile grains partially exposed to the light: towards a new tool for single grain OSL dating of poorly bleached mortars. Radiat. Meas. 107, 48–57. http://dx.doi.org/10.1016/j.radmeas.2017.10.003.
Hajdas, I., Lindroos, A., Heinemeier, J., Ringbom, A., Marzaioli, F., Terrasi, F., Passariello, I., Capano, M., Artioli, G., Addis, A., Secco, M., Michalska, D., Czernik, J., Goslar, T., Hayen, R., Van Strydonck, M., Fontaine, L., Boudin, M., Maspero, F., Panzeri, L., Galli, A., Urbanová, P., Guibert, P., 2017. Preparation and dating of mortar samples - Mortar Dating Inter-comparison Study (MODIS). In: Radiocarbon 59–5, p. 1–14, Selected Papers from the 8th Radiocarbon & Archaeology Symposium, Edinburgh, UK, 27 June-1 July 2016, http://dx.doi.org/10.1017/RDC.2017.112.
Hayen, R., Van Strydonck, M., Fontaine, L., Boudin, M., Lindroos, A., Heinemeier, J., Ringbom, Å., Michalska, D., Hajdas, I., Hueglin, S., Marzaioli, F., Terrasi, F., Passariello, I., Capano, M., Maspero, F., Panzeri, L., Galli, A., Artioli, G., Addis, A., Secco, M., Boaretto, E., Ch, Moreau, Guibert, P., Urbanová, P., Czernik, J., Goslar, T., 2017. Mortar dating methodology: intercomparison of available methods. In: Radiocarbon 59–6, p. 1859–1871, Selected Papers from the 8th Radiocarbon & Archaeology Symposium, Edinburgh, UK, 27 June-1 July 2016, http://dx.doi.org/10.1017/RDC.2017.129.
Heinemeier, J., Jungner, H., Lindroos, A., Ringbom, Å., von Konow, T., Rud, N., 1997. AMS 14C dating of lime mortar. Nucl. Inst. Methods Phys. Res. B 123 (1–4), 487–495.
Heinemeier, J., Ringbom, A., Lindroos, A., Sveinbjornsdottir, A.E., 2010. Successful AMS -C14 dating of non-hydraulic lime mortars from the medieval churches of the Aland Islands, Finland. Radiocarbon 52/1, 171–204.
Jain, M., Thomsen, K.J., Bøtter-Jensen, L., Murray, A.S., 2004. Thermal transfer and apparent-dose distributions in poorly bleached mortar samples: results from single grains and small aliquots of quartz. Radiat. Meas. 38, 101–109. http://dx.doi.org/10.1016/j.radmeas.2003.07.002.
Kim, J.C., Roberts, H.M., Duller, G.A.T., Lee, Y.I., Yi, S.B., 2009. Assessment of diagnostic tests for evaluating the reliability of SAR *De* values from polymineral and quartz fine grains. Radiat. Meas. 44 (2), 149–157. http://dx.doi.org/10.1016/j.radmeas.2009.01.003.
Labeyrie, J., Delibrias, G., 1964. Dating of old mortars by the carbon-14 method. Nature 201, 742.
Lanos, P., 1998. L'archéomagnétisme. In: Ferdière, A. (Ed.), Les Méthodes de Datation en Laboratoire, pp. 166–184 (Collection « Archéologiques », Edition Errance, Paris).
Lanos, P., Philippe, A., 2017. Hierarchical Bayesian modeling for combining dates in archaeological context. J. de la Société Française de Statistique 158 (2), 72–88. http://journal-sfds.fr/index.php/J-SFdS/issue/view/68.
Lanos, P., Kovacheva, M., Chauvin, A., 1999. Archaeomagnetism, methodology and applications: implementation and practice of the archaeomagnetic method in France and Bulgaria. Eur. J. Archaeol. 2 (3), 365–392.
Lanos, P., Philippe, A., Lanos, H., Dufresne, P., 2015. Chronomodel: chronological modelling of archaeological data using Bayesian Statistics ((Version 1.1). Available from). http://www.chronomodel.fr.
Lanos, P., Philippe, A., Lanos, H., Dufresne, P., 2016. Chronomodel: chronological modelling of archaeological data using Bayesian Statistics ((Version 1.5). Available from). https://chronomodel.com.
Lindroos, A., Heinemeier, J., Ringbom, Å., Braskén, M., Sveinbjörnsdóttir, Á., 2007. Mortar dating using AMS 14C and sequential dissolution: examples from medieval, nonhydraulic lime mortars from the Åland Islands, SW Finland. Radiocarbon 49/1, 47–67.
Maillé, M., 1960. Recherches sur les origines chrétiennes de Bordeaux, Paris.
Martin, L., Mercier, N., Incerti, S., Lefrais, Y., Pecheyran, C., Guérin, G., Jarry, M., Bruxelles, L., Bon, F., Pallier, C., 2015. Dosimetric study of sediments at the beta dose rate scale: characterization and modeli-zation with the DosiVox software. Radiat. Meas. 81, 134–141. http://dx.doi.org/10.1016/j.radmeas.2015. 02.008.
Marzaioli, F., Nonni, S., Passariello, I., Capano, M., Ricci, P., Lubritto, C., De Cesare, N., Eramo, G., Castillo, J.A.Q., Terrasi, F., 2013. Accelerator mass spectrometry ^{14}C dating of lime mortars: methodological aspects and field study applications at CIRCE (Italy). Nucl. Inst. Methods Phys. Res. B 294, 246–251.
Michel, A., 2012. Autour de l'identification des mausolées: le cas de Saint-Seurin de Bordeaux. In: Mausolées & Églises, IVe-VIIIe siècle, Hortus Artium Medievalium, (18/2, 2012).
Michel, A., 2014. La crypte de la basilique Saint-Seurin, commune de Bordeaux. In: Rapport d'Opération Archéologique, (relevés stratigraphiques effectuées du 12 au 18/5, du 16 au 20/6 et les 1/7 et 3/7/2014).
Michel, A., Cartron, I., Piat, J.-L., 2009. Saint Seurin de Bordeaux: Etude archéologique de la crypte: observations préliminaires. In: Cartron, I., Barraud, D., Henriet, P., Michel, A. (Eds.), Autour de Saint-Seurin: lieu, mémoire, pouvoir, des premiers temps chrétiens à la fin du Moyen Âge, Actes de colloque de Bordeaux 12-14/10/2009, Bordeaux, pp. 197–233 (351 p., Ausonius éditions, ISBN: 978-2-35613-012-2-9).
Miriello, D., Barca, D., Bloise, A., Ciarallo, A., Crisci, G.M., 2010. Characterization of archaeological mortars from Pompeii (Campania, Italy) and identification of construction phases by compositional data analysis. J. Archaeol. Sci. 37, 2207–2223.
Murray, A.S., Olley, J.M., 2002. Precision and accuracy in the optically stimulated luminescence dating of sedimentary quartz: a status review. Geochronometria 21, 1–16.
Murray, A.S., Wintle, A., 2000. Luminescence dating of quartz using an improved single-aliquot regenerative dose protocol. Radiat. Meas. 32, 523–538.
Nawrocka, D., Michniewicz, J., Pawlyta, J., Pazdue, A., 2005. Application of radiocarbon method for dating of lime mortars. Geochronometria 24, 109–115.
Ortega, L.A., Cruz Zuluaga, M., Alonso-Olazabal, A., Insausti, M., Murelaga, X., Ibañez, A., 2012. Improved sample preparation methodology on lime mortar for reliable ^{14}C dating. In: Nawrocka, Danuta Michalska (Ed.), Radiometric Dating. 978-953-51-0596-1, .
Panzeri, L., 2013. Mortar and surface dating with optically stimulated luminescence (OSL): innovative techniques for the age determination of buildings. Nuovo Cimento della 36 (4), 205–216.
Pesce, G., Ball, R.J., 2000. Dating of old lime based mixtures with the pure lime lumps technique. In: Nawrocka, D.M. (Ed.), Radiometric Dating. InTech, 2012, pp. 21–39.
Reimer, P., Bard, E., Bayliss, A., Beck, J., Blackwell, P., Ramsey, C.B., et al., 2013. IntCal13 and Marine13 radiocarbon age calibration curves 0–50,000 years cal BP. Radiocarbon 55 (4), 1869–1887.
Ringbom, Å., Heinemeier, J., Lindroos, A., Brock, F., 2011. Mortar dating and Roman pozzolana: Results and interpretations. In: Commentationes Humanarum Litterarum. 128. Societas Scientiarum Fennica, pp. 187–208.
Roberts, H.M., Wintle, A.G., 2001. Equivalent dose determinations for polymineralic fine-grains using the SAR protocol: application to a Holocene sequence of the Chinese Loess Plateau. Quat. Sci. Rev. 20 (5–9), 859–863. http://dx.doi.org/10.1016/S0277-3791(00)00051-2.
Rougé, G., Scuiller, C., Gleize, Y., 2015. Cartographie des sites à sarcophages en Aquiaine (IVe-VIIIe siècles). In: Les sarcophages de l'Antiquité Tardive et du aut Moyen Age: Fabrication, Utilisation, Diffusion. Proceedings of International Conference, Bordeaux 2009, pp. 149–154 (ISBN: 2-910763-40-4, Aquitania).
Sanjurjo-Sánchez, J., Trindade, M.J., Blanco-Rotea, R., Benavides Garcia, R., Fernández Mosquera, D., Burbidge, C., Prudêncio, M.I., Dias, M.I., 2010. Chemical and mineralogical characterization of historic mortars from the Santa Eulalia de Bóveda temple, NW Spain. J. Archaeol. Sci. 37, 2346–2351.
Sapin, C., 1991. Enduits et Mortiers. Archéologie Médiévale et Moderne. Dossier de documentation archéologique, Paris, CNRS, pp. 15.
Stella, G., Fontana, D., Gueli, A.M., Troja, S.O., 2013. Historical mortars dating from OSL signals of fine grain fraction enriched in quartz. Geochronometria 40 (3), 153–164. http://dx.doi.org/10.2478/s13386-013-0157-y.
Stella, G., Fontana, D., Gueli, A.M., Troja, S.O., 2014. Different approaches to date bricks from historical buildings. Geochron 41–3, 256–264. http://dx.doi.org/10.2478/s13386-013-0157-y.
Thellier, E., Thellier, O., 1959. Sur l'intensité du champ magnétique terrestre dans le passé historique et géologique. Annales de Géophysique 15 (3), 285–376.
Thomsen, K.J., Murray, A., Bøtter-Jensen, L., 2005. Sources of variability in OSL dose measurements using single grains of quartz. Radiat. Meas. 39, 47–61.
Thomsen, K.J., Murray, A.S., Bøtter-Jensen, L., Kinahan, J., 2007. Determination of burial dose in incompletely bleached fluvial samples using single grains of quartz. Radiat. Meas. 42 (3), 370–379.
Thomsen, K.J., Murray, A., Jain, M., 2012. The dose dependency of the over-dispersion of quartz OSL single grain dose distributions. Radiat. Meas. 47, 732–739.
Tubbs, L.E., Kinder, T.N., 1990. The use of AMS for the dating of lime mortars. Nucl. Instrum. Methods Phys. Res., Sect. B 52 (3–4), 438.
Turney, C.S.M., Flannery, T.F., Roberts, R.G., Reid, C., Fifield, L.K., Higham, F.G., Jacobs, Z., Kemp, N., Colhoun, E.A., Kalin, R.M., Ogle, N., 2008. Late-surviving megafauna in Tasmania, Australia, implicate human involvement in their extinction. Proc. Natl. Acad. Sci. U. S. A. 105, 12150–12153.
Urbanová, P., Guibert, P., 2017. A methodological study on single grain OSL dating of mortars: comparison of five reference archaeological sites. Geochronometria 44, 77–97. http://dx.doi.org/10.1515/geochr-2015-0050.

Urbanová, P., Hourcade, D., Ney, C., Guibert, P., 2015. Sources of uncertainties in OSL dating of archaeological mortars: the case study of the Roman amphitheatre *Palais-Gallien* in Bordeaux. Radiat. Meas. 72, 100–110.
Vendrell-Saz, M., Alarcon, S., Molera, J., Garcia-Valles, M., 1996. Dating ancient lime mortars by geochemical and mineralogical analysis. Archaeometry 38 (1), 143–149.
Zacharias, N., Mauz, B., Michael, C.T., 2002. Luminescence quartz dating of lime mortars. A first research approach. Radiat. Prot. Dosim. 101, 379–382.
Zhang, J.F., Fan, C.F., Wang, H., Zhou, L.P., 2007. Chronology of an oyster reef on the coast of Bohai Bay, China: constraints from op-tical dating using different luminescence signals from fine quartz and polymineral fine grains of coastal sediments. Quat. Geochronol. 2 (1–4), 71–76. http://dx.doi.org/10.1016/j.quageo.2006.05.027.